DOI: 10.1002/ejic.201100334

An Easy Route to Pure and Luminescent Eu-Doped YVO_4 Polycrystalline Films Based on Molecular or Hybrid Precursors

Nicolas Deligne,[a] Julien Lamme,[a] and Michel Devillers*[a]

Keywords: Yttrium / Vanadium / Europium / Luminescence / Thin films

An easy "soft-chemistry" method has been developed to prepare pure and luminescent Eu-doped YVO_4 films. The method is based on the spin-coating of aqueous solutions of stoichiometrically well-defined yttrium(III)– and/or dioxidovanadium(V)–edta complexes, sometimes in the presence of a cellulose derivative, namely (hydroxypropyl)methyl cellulose. Films of the corresponding binary oxides, Y_2O_3 and V_2O_5, were also studied for comparative purposes. XRD, Raman spectroscopy and scanning electron microscopy were used to characterize the samples at different stages of their preparation. The spin-coating rate as well as the presence of the cellulose derivative in the precursor solutions were found to influence greatly the homogeneity and morphology of the films. The preferential orientation of crystallites within some of the films was also evidenced.

Introduction

Inorganic materials based on oxides or metallates exhibit a wide range of physical and chemical properties, which justifies the search for simple and easy preparation routes, either as powders or as thin films. Yttrium sesquioxide, Y_2O_3, has attracted much attention because of its high thermal conductivity, high refractive index and high dielectric constant associated with an upper band gap.[1] Pure and doped Y_2O_3, among others, have been studied as dielectric layers for electroluminescent devices and as planar optical waveguiding thin films. Y_2O_3 is also an interesting phosphor host matrix.[2] Vanadium pentoxide, V_2O_5, is also a promising material, especially in the form of thin films, because of its multicoloured electrochromism, wide optical band gap and excellent thermoelectric properties.[3] These properties make V_2O_5 an ideal candidate for various applications, such as gas sensing, catalysis, solar cells and thin-film batteries. The mixed Y/V compound, yttrium orthovanadate, YVO_4, is particularly attractive as a host matrix for lanthanide ions in the field of luminescence. Eu^{3+}-doped YVO_4 was first proposed by Levine and Palilla as a phosphor for colour television tubes and was subsequently used for a long time in such devices.[4]

Thin films of V_2O_5, Y_2O_3 and YVO_4 can be prepared by quite different sophisticated techniques such as direct current or radio frequency magnetron sputtering, chemical vapour deposition and pulsed laser deposition.[5] They can also be obtained by sol–gel methods[2,6] or Pechini sol–gel processes,[7] and recently a polymer-assisted deposition technique was used to prepare Eu^{3+}-doped YVO_4.[8] YVO_4:Eu films have also been deposited on glass and Si(100) slides by using a microwave-assisted chemical solution deposition technique.[9] More recently, Wang et al. fabricated YVO_4:Eu films on a quartz substrate by soft lithography.[10]

In this work, Y_2O_3, V_2O_5, YVO_4 and YVO_4:Eu films were prepared by a chemical method based essentially on stoichiometrically well-defined and water-soluble coordination complexes that make the process easy, perfectly controlled and widely applicable to other related formulations. The films were deposited on quartz substrates by spin-coating of an aqueous solution of edta compounds, then dried and calcined under appropriate but rather mild conditions when compared with other routes. (Hydroxypropyl)methyl cellulose (HPMC) was added to a series of samples of the spin-coating solution, and its effect on the structural and morphological properties of the films was investigated. The purpose of using this additive was to modulate the viscosity of the spin-coating solutions. According to spin-coating theory, the viscosity is indeed an important parameter influencing mainly the radial flow of liquid during the spin-coating process.[11] Recently, some authors have used ethyl cellulose or ethylene glycol and citric acid to investigate the impact of the viscosity of precursor solutions.[12] These studies have shown that the morphology and particularly the number of cracks, the roughness and the thickness of the films are greatly affected by this parameter. In addition, blends of water-soluble HPMC and water-insoluble ethyl cellulose have been used in the formulation of drug delivery film coatings.[13] To the best of our knowledge, although it has been used in drug delivery systems, HPMC has almost

[a] Institute of Condensed Matter and Nanosciences, Université Catholique de Louvain,
Place Louis Pasteur 1, 1348 Louvain-la-Neuve, Belgium
Fax: +32-10-472330
E-mail: michel.devillers@uclouvain.be

Supporting information for this article is available on the WWW under http://dx.doi.org/10.1002/ejic.201100334.

never been used for the synthesis of inorganic films such as oxides or metallates by a spin-coating process.[14] Nevertheless, some authors have reported the preparation of nickel-based conducting films from coordination compounds and various cellulose-based additives.[14a] This is a little surprising considering the interesting properties of this polymer in these kinds of applications. In contrast, HPMC has recently been used for the preparation of multicationic oxides such as $La_{0.9}Sr_{0.1}Ga_{0.8}Mg_{0.2}O_{2.85}$ and $LiNi_{0.5}Mn_{0.5}O_2$.[15] In these studies, HPMC was implemented in successive freeze-drying and self-ignition processes.

Results and Discussion

Complexes were prepared according to a published procedure and were fully characterized.[16] Chemical composition, purity and water content were determined by elemental analysis, thermogravimetric analysis, ^1H, ^{13}C NMR and FTIR spectrosopy, and mass spectrometry.

In this work, different systems were investigated. First, films were prepared by spin coating of an aqueous solution containing only one coordination compound, namely either $(NH_4)[Y^{III}(edta)]\cdot 6H_2O$ or $(NH_4)_3[V^V(O)_2(edta)]\cdot 0.5H_2O$. Secondly, films containing both Y- and V-based complexes were prepared by the spin coating of a homogeneous mixture of the aqueous complex solutions. In all cases, the films were characterized before and after calcination. In this paper, they are called "precursor films" and "oxide films", respectively (see Figure 12). In addition, all the systems were prepared either with HPMC as additive in the spin-coating solution or without HPMC. Finally, Eu^{3+}-doped YVO_4 films were also prepared from a mixed solution containing $(NH_4)[Y^{III}(edta)]\cdot 6H_2O$, $(NH_4)[Eu^{III}(edta)]\cdot 7.5H_2O$ and $(NH_4)_3[V^V(O)_2(edta)]\cdot 0.5H_2O$ in appropriate proportions.

Precursor Films

$(NH_4)[Y(edta)]\cdot xH_2O$

Films prepared from an aqueous solution of $(NH_4)[Y^{III}(edta)]\cdot 6H_2O$ were characterized by X-ray diffraction before any further treatment to evidence the presence of the complex on the quartz substrate. Figure 1 shows the results obtained without cellulose additive.

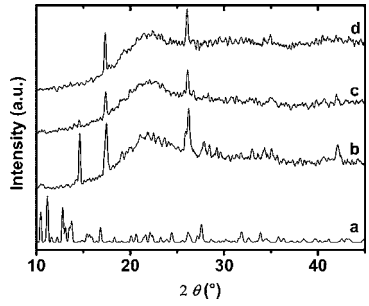

Figure 1. XRD patterns of (a) bulk $(NH_4)[Y(edta)]\cdot 6H_2O$ and $(NH_4)[Y(edta)]\cdot xH_2O$ precursor films prepared by the spin coating of an HPMC-free solution at (b) 1000, (c) 2000 and (d) 3000 rpm.

As evidenced by the presence of sharp peaks in the XRD pattern of the bulk complex, the synthesized coordination compound $(NH_4)[Y^{III}(edta)]\cdot 6H_2O$ is crystalline (Figure 1a). As expected, sharp lines were also observed in the XRD curves of the films, but they do not correspond to the most intense lines observed for the bulk compound, which indicates that different crystallographic structures are present in two cases. This can be easily understood as water molecules play a major role in the stabilization of the crystal structure and also because the parameters governing the crystallization process in the bulk powder synthesis and film preparation are clearly different. The number of water molecules in the film is therefore probably not the same as in the bulk sample. In addition, a drying step is carried out on the film after coating that influences the water content.

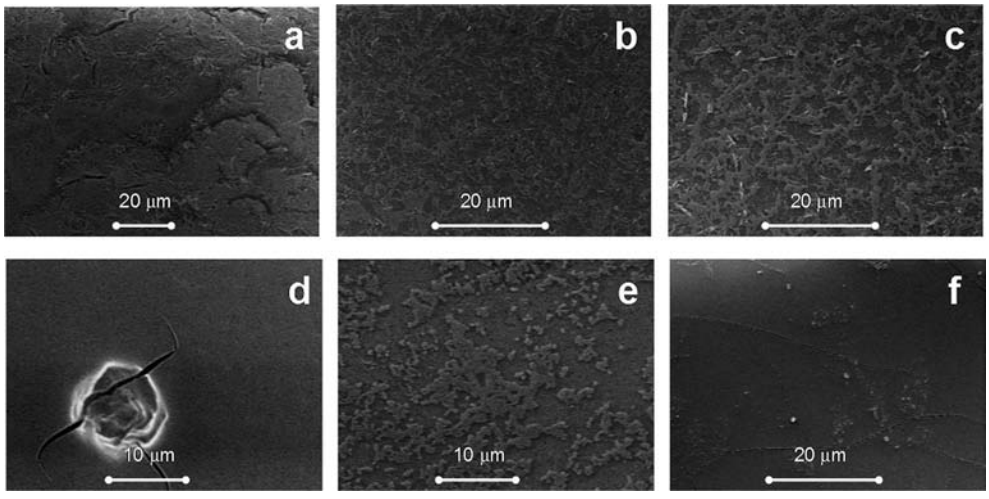

Figure 2. SEM pictures of films prepared by spin coating of an $(NH_4)[Y^{III}(edta)]\cdot xH_2O$ solution without HPMC at (a) 1000, (b) 2000 and (c) 3000 rpm and with HPMC at (d) 1000, (e) 2000 and (f) 3000 rpm.

However, this step does not seem to be the driving force for the modification of the crystal structure. The XRD pattern of the complex is indeed unchanged when the powder is dried at 110 °C. The diffractograms of the $(NH_4)[Y^{III}(edta)]\cdot xH_2O$ films prepared in the presence of HPMC were also recorded, but unfortunately no signals were detected, which indicates that the films are either amorphous or too thin to give a sufficiently high signal. Raman spectroscopy was also used to analyse these films but again no signal was obtained irrespective of whether HMPC was used or not.

Each film was then characterized by scanning electron microscopy. As illustrated in Figure 2 for $(NH_4)[Y^{III}(edta)]\cdot xH_2O$ films prepared with and without HPMC, the spin-coating rate significantly influences the morphology of the films. In addition, when HPMC is used in the spin-coated solutions, the morphology of the films appears to be completely different. In this case, at 1000 rpm, an homogeneous layer is obtained with no voids, but many cracks are present (Figure 2d). At 2000 rpm, the number of voids increases and at 3000 rpm a homogeneous film with some cracks is observed.

$(NH_4)_3[V(O)_2(edta)]\cdot xH_2O$

Films of the dioxidovanadium(V) complex were prepared on quartz substrates by using various spin-coating rates, with or without HPMC. Figure 3 shows the XRD results obtained when the films were prepared from a solution of $(NH_4)_3[V(O)_2(edta)]$ without HPMC. Interestingly, as for the Y^{3+} complex, the XRD patterns of the films are rather different to that obtained for the bulk compound. This confirms that the crystallization process is strongly affected by the preparation method. Again, the subsequent drying step at 110 °C does not seem to be the driving force for the change in the crystal structure.

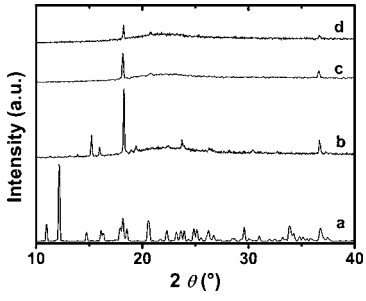

Figure 3. XRD patterns of (a) bulk $(NH_4)[V(O)_2(edta)]\cdot 0.5H_2O$ and $(NH_4)[V(O)_2(edta)]\cdot xH_2O$ precursor films prepared by the spin coating of a HPMC-free solution at (b) 1000, (c) 2000 and (d) 3000 rpm.

The XRD patterns of the films prepared from HPMC-based solutions are quite different (Supporting Information, Figure S1). The only diffraction peak observed in the XRD curves of these films corresponds to the most intense peak of the bulk sample. This suggests that, in this case, the crystal structure of the complex $(NH_4)[V(O)_2(edta)]\cdot 0.5H_2O$ is nearly the same whether on the quartz substrate or in the powder. A slight shift is, however, observed for the film prepared at 1000 rpm, which suggests small structural differences between the bulk and spin-coated complex in this case. The significant difference in the XRD results obtained with the HPMC-free and HPMC-based films suggests that, at least for this complex, the crystallization process occurs differently in the absence or presence of the additive.

Raman spectroscopy was used to characterize the films and prove the presence of the complex on the support. Figure 4 shows the results obtained for samples prepared without HPMC. The film prepared at 3000 rpm does not exhibit any Raman signal, except for broad bands at around 1000, 850 and 700 cm^{-1}, which have been assigned to the quartz support. The absence of Raman signals is probably linked to either the presence of many voids or to the formation of films that are too thin. Raman spectra were also recorded for samples prepared at 1000 and 2000 rpm; these were identical in all cases but quite different to that of the bulk complex. More particularly, the V–O stretching, which appears at around 900 cm^{-1} in the bulk sample, is shifted to about 970 cm^{-1} in the films. This must be related to the variation of the crystal structure in the bulk and the films shown by XRD (Figure 3). For HPMC-based films, the results are the same, namely the absence of a signal for the sample prepared at 3000 rpm and an unexpected Raman feature for the samples prepared at 1000 and 2000 rpm (Figure S2). Even if, according to the XRD patterns, HPMC-based films have almost the same crystal structure as the bulk sample, small deviations from the original symmetry could cause an allowed transition to become forbidden, and vice versa. In addition, small modifications of the V–O bond length can lead to a significant shift in the position of the V=O stretching band. Its position is indeed really sensitive to the symmetry and the V–O bond length, with this vibration mode having been observed in the range of 1050 to 900 cm^{-1} in different molecules.[17] The role of water molecules can also be invoked as partially responsible for the shift. Some authors have reported a rocking band of coordinated water molecules at around 820 cm^{-1} in a (malonato)vanadium(IV) complex.[18] In our case, this band also seems to be present in the vanadium(V) complex but disappears in the Raman spectra of the films. The drying

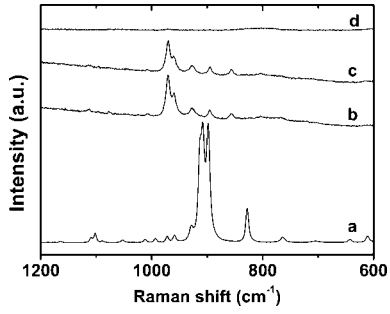

Figure 4. Raman spectra of (a) bulk $(NH_4)[V(O)_2(edta)]\cdot 0.5H_2O$ and $(NH_4)[V(O)_2(edta)]\cdot xH_2O$ precursor films prepared by the spin coating of a HPMC-free solution at (b) 1000, (c) 2000 and (d) 3000 rpm.

step is most probably responsible for this. The elimination of involved water molecules during the process can lead to a shift in the V=O Raman band.

Scanning electron microscopy was used to characterize the morphology of the films (Figures S3 and S4). It appears from these results that the number of voids within the films increases with the spin-coating rate. This is consistent with previous literature on bismuth molybdate films.[17] In addition, the use of HPMC strongly influences the morphology.

Mixed Precursor Films

Films containing both yttrium and vanadium were prepared by the spin coating of a homogeneous mixture of aqueous solutions of the corresponding complexes and characterized by XRD. For almost all samples, the XRD signals were too low except for films prepared at low spin-coating rates without HPMC, as shown in Figure 5. For the film prepared at 1000 rpm without HPMC (Figure 5c), the XRD pattern corresponds neither to one of the two complexes involved (Figure 5a and b) nor to a mixture of these two complexes. Neither does it correspond to the XRD pattern of the vanadium complex film observed in Figure 3. As for the monometallic precursor films, the crystal structure of the coordination compound present within the film is concluded to be different to that in the bulk.

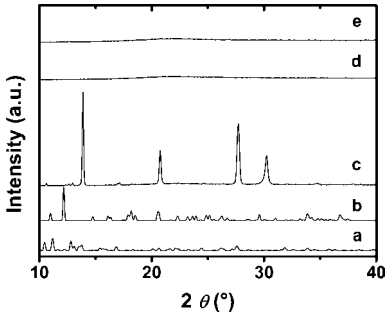

Figure 5. XRD patterns of (a) bulk $(NH_4)[V(O)_2(edta)]\cdot 0.5H_2O$, (b) bulk $(NH_4)[Y(edta)]\cdot 6H_2O$ and Y/V precursor films prepared by the spin coating of an HPMC-free solution at (c) 1000, (d) 2000 and (e) 3000 rpm.

The Raman spectra of these HPMC-free films were also recorded (Figure S5). It is clear that the Raman spectrum of the film prepared at 1000 rpm corresponds to that of the yttrium(III) complex. This suggests either that the film is inhomogeneous or that, within the film, the yttrium complex is crystalline, whereas the vanadium complex is amorphous, based on the known influence of amorphicity on Raman intensity. When the film is spin-coated at 2000 rpm, the Raman spectrum is different and corresponds neither to that of the bulk Y^{3+} complex nor to a mixture of both complexes. Finally, when the highest spin-coating rate was used, no signal at all was detected, which shows either that the amount of material is too small or that the complexes are amorphous.

The morphology of the mixed precursor films was studied by SEM. For HPMC-free films, the results again indicate that the spin-coating rate influences strongly the morphology (Figure S6). The film prepared by spin coating at 1000 rpm contains sticks of various sizes, whereas films prepared at 2000 and 3000 rpm consist of a thin precursor layer containing voids. The presence of sticks on the 1000 rpm spin-coated plate was observed neither in the $(NH_4)_3[V(O)_2(edta)]\cdot xH_2O$ films nor in the $(NH_4)[Y^{III}(edta)]\cdot xH_2O$ films. This particular morphology could explain the specific XRD pattern obtained for this mixed precursor (Figure 5c). When HPMC is added to the spin-coated solution, the resulting films appear to have a different morphology, in particular those obtained at low spin-coating rates (Figure S7). SEM images of the film prepared at 1000 rpm indicate the presence of a uniform layer with many cracks. This morphology is similar to that obtained for the $(NH_4)_3[V(O)_2(edta)]\cdot xH_2O$ and $(NH_4)[Y^{III}(edta)]\cdot xH_2O$ films prepared under the same conditions. At 2000 rpm, the film seems to be homogeneous with a few cracks and no voids, whereas a spinning rate of 3000 rpm leads to a film with many of voids and no cracks. With the exception of the 1000 rpm HPMC-free film, all these results are consistent with the results obtained with the monometallic precursor films.

Thermal Behaviour of the Molecular Precursors

To determine the appropriate calcination conditions for the preparation of the oxide films, the thermal behaviour of the precursors was studied. For this purpose, solutions containing the coordination complexes with and without HMPC were freeze-dried, and the resulting solids were studied by thermogravimetric analysis. For the monometallic precursors, the results indicate that the final decomposition temperature lies at around 500 °C for the vanadium precursor and at over 700 °C for the yttrium precursor. According to these results, the precursor films were calcined for 2 h at 600 °C for V_2O_5 and at 800 °C for Y_2O_3. For mixed Y/V/O systems, the final decomposition temperature of both the HPMC and HPMC-free precursors lies at around 600 °C. However, XRD analyses indicate the presence of small amounts of binary oxides at 500 and 600 °C when the HPMC-free precursor is used. According to these analyses, the temperature of 800 °C is required to provide a highly crystalline and pure material. This is not the case when the HPMC precursor is used as a temperature of 600 °C is sufficient to produce pure YVO_4. Therefore, for YVO_4 films, a temperature of 600 °C was selected in the presence of HPMC, whereas HPMC-free precursors were heated at 800 °C.

Oxide Films

Y_2O_3 Films

According to the TG analysis performed on the bulk complex, the $(NH_4)[Y^{III}(edta)]\cdot xH_2O$ films were calcined at 800 °C for 2 h. After calcination, the Y_2O_3 films were char-

acterized by XRD. In most cases, the XRD signal was too low to identify the oxide phase. However, when XRD curves of the films prepared without HPMC are compared with the XRD pattern of bulk Y_2O_3 (Figure S8), typical diffraction peaks of Y_2O_3 are observed (JCPDS-ICDD file 41-1105) only when a spin-coating rate of 1000 rpm is used. For Y_2O_3 films prepared with HPMC, a detectable XRD pattern was obtained only at a spinning rate of 3000 rpm (Figure S9), but this did not match that of bulk Y_2O_3, which indicates another structure.

Films prepared without HPMC were characterized by Raman spectroscopy, and a typical Raman band from Y_2O_3 at 378 cm^{-1} is observed at a spin-coating rate of 1000 rpm (Figure S10). For other spin-coating rates, only the Raman spectrum of the quartz support can be detected. When HPMC-based solutions are used, the Raman spectra of Y_2O_3 films do not exhibit any signal.

If we compare the SEM pictures obtained for Y_2O_3 films prepared with and without HPMC, it is clear that the use of HPMC induces the formation of more dense and more uniform films for all spin-coating rates (Figure S11).

V_2O_5 Films

In accord with the TG analysis, $(NH_4)[V(O)_2(edta)]\cdot xH_2O$ films were calcined at 600 °C for 2 h. The XRD patterns of the films prepared without HPMC (Figure 6) exhibit few diffraction peaks that correspond only to the 00*l* reflections of the α-V_2O_5 oxide (JCPDS-ICDD file 41-1426). This suggests that V_2O_5 crystals within the films are not randomly oriented but are preferentially oriented along the *c* axis perpendicular to the substrate surface. The same behaviour is observed for V_2O_5 films prepared from HPMC-based solutions (Figure S12). Again, 00*l* diffraction peaks are detected, whereas peaks associated with other Miller indices are almost invisible.

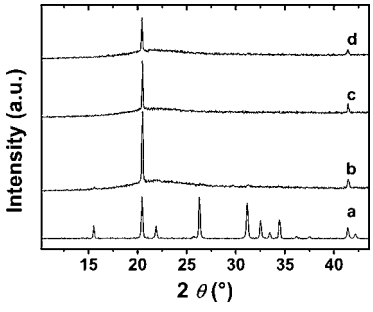

Figure 6. XRD patterns of (a) bulk V_2O_5 (I/8) and V_2O_5 films prepared by spin coating of an HPMC-free solution at (b) 1000, (c) 2000 and (d) 3000 rpm.

The Raman spectra of the films prepared from HPMC-free solutions are shown in Figure 7. In most cases, the recorded spectra exhibit typical Raman bands of V_2O_5. However, at 3000 rpm, only the Raman signal from the quartz plate is observed, which indicates very thin films. The same results are obtained for films prepared from HPMC-based solutions (Figure S13).

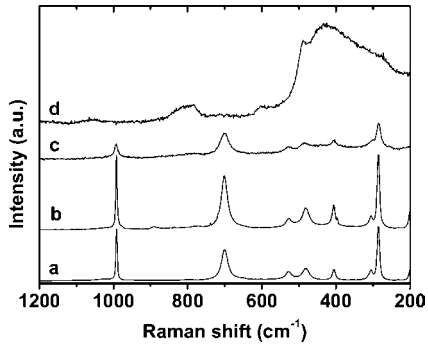

Figure 7. Raman spectra of (a) bulk V_2O_5 (I/20) and V_2O_5 films prepared by the spin coating of an HPMC-free solution at (b) 1000 (I/20), (c) 2000 and (d) 3000 rpm and calcined at 600 °C for 2 h.

As evidenced by SEM, V_2O_5 films exhibit different kinds of morphologies (Figure 8). Depending on the preparation conditions, scanning electron microscopy reveals the presence of sticks or filaments of various sizes as well as spherical particles. In addition, for a series of samples, these diverse morphologies can be seen together on one film simultaneously. It appears that the addition of HPMC limits this phenomenon, the films being more homogeneous on the microscopic scale with the formation of spherical particles being favoured.

YVO_4 Films

Mixed precursor films containing both $(NH_4)[V(O)_2(edta)]\cdot xH_2O$ and $(NH_4)[Y(edta)]\cdot xH_2O$ were calcined at 600 or 800 °C for HPMC-based and HPMC-free samples, respectively. The XRD patterns for each film prepared without HPMC are shown in Figure 9. The XRD peaks, usually of very low intensity, can be assigned to the zircon-type tetragonal YVO_4 phase (JCPDS-ICDD file 17-0341). The relative intensities of the XRD peaks in the 1000 rpm spin-

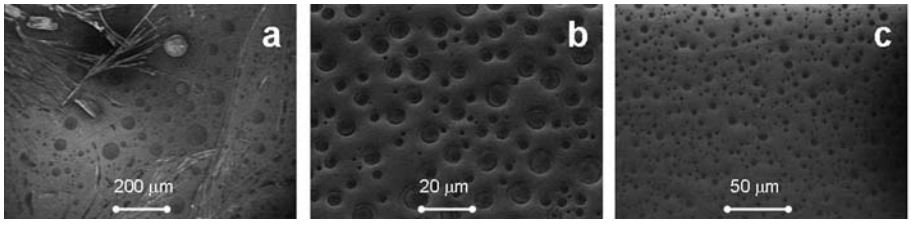

Figure 8. SEM pictures of V_2O_5 films prepared by the spin coating of an HPMC-free solution at (a) 1000 rpm and by the spin coating of an HPMC-based solution at (b) 1000 and (c) 3000 rpm.

coated film suggest at least a partial preferential orientation of crystallites (Figure 9b). Compared with the bulk XRD pattern, diffraction peaks associated with the 200 ($2\theta \approx 25°$) and 400 ($2\theta \approx 52°$) reflections are indeed overexpressed in comparison with the other lines. This suggests that the crystallites are oriented along the *a* axis perpendicular to the substrate surface. When HPMC is used and with a spin-coating rate of 1000 rpm, the most intense diffraction peak of bulk YVO_4 is observed (Figure S14). For other spin-coating rates, the XRD signals are almost negligible.

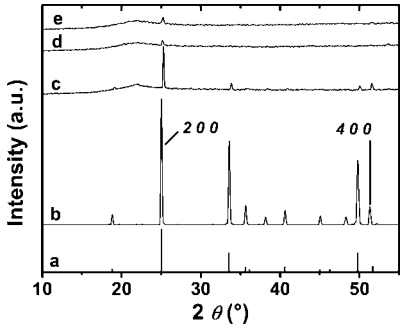

Figure 9. XRD patterns of (a) JCPDS-ICDD file 17-0341, (b) bulk YVO_4 (I/8) and YVO_4 films prepared by the spin coating of an HPMC-free solution at (c) 1000, (d) 2000 and (e) 3000 rpm.

As shown in Figure 10 for films prepared from HPMC-based solutions, Raman spectroscopy confirmed the presence of YVO_4. The results obtained for films prepared without HPMC are presented in the Supporting Information (Figure S15).

As illustrated in Figure 11a, the SEM image obtained for an HPMC-free solution spin-coated at 1000 rpm shows a highly inhomogeneous film in terms of morphology. Increasing the spin-coating rate allows the formation of more uniform films, but a number of voids are observed (Figure 11b and c). When HPMC-based solutions are spin-coated, the homogeneity is improved with less voids even at low spin-coating rates, as shown in Figure 11d–f.

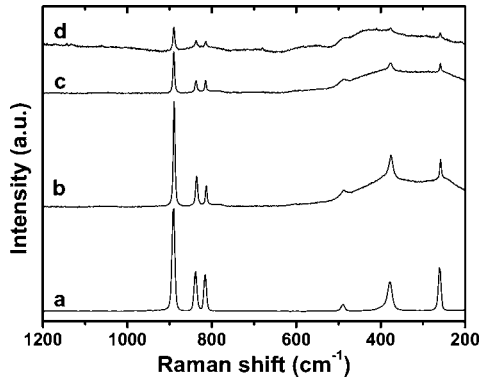

Figure 10. Raman spectra of (a) bulk YVO_4 (I/8) and YVO_4 films prepared by the spin coating of an HPMC-based solution at (b) 1000, (c) 2000 and (d) 3000 rpm.

Eu^{3+}-Doped YVO_4 Films

From a mixed solution containing $(NH_4)[Y^{III}(edta)]\cdot 6H_2O$, $(NH_4)[Eu^{III}(edta)]\cdot 7.5H_2O$ and $(NH_4)_3[V^{V}(O)_2(edta)]\cdot 0.5H_2O$, mixed Y/Eu/V films were prepared with or without HPMC and were calcined to produce YVO_4:Eu films (Eu is the doping element with a ratio equal to 4 mol-% in comparison with yttrium). Emission spectra were recorded for bulk YVO_4:Eu and films prepared at 3000 rpm and, for each sample, emission bands are observed that are characteristic of Eu^{3+} in a D_{2d} site, as expected for a tetragonal zircon-type phase (Figure S16).

To visualize the luminescence properties of the films, macroscopic pictures were taken by using a conventional photo camera. The characteristic red emission of YVO_4:Eu was observed under UV irradiation for films prepared from HPMC-free and HMPC-based solutions. It is clear that the use of HPMC has a great impact on the macroscopic homogeneity of the films. In particular, an HPMC-based solution spin-coated at 3000 rpm leads to a highly homogeneous film at the macroscopic level (Figure S17).

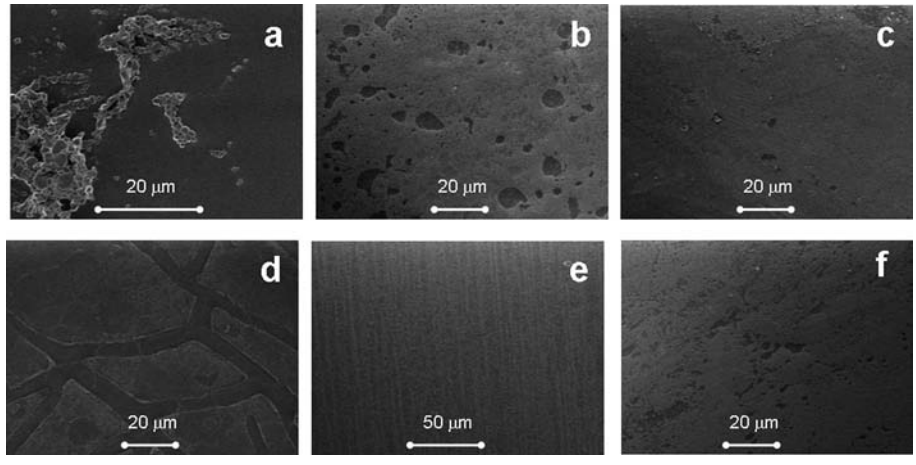

Figure 11. SEM images of YVO_4 films prepared by the spin coating of an HPMC-free solution at (a) 1000, (b) 2000 and (c) 3000 rpm and by the spin coating of an HPMC-based solution at (d) 1000, (e) 2000 and (f) 3000 rpm.

Conclusions

In this work, an easy, inexpensive and comparatively "soft-chemistry" method involving the spin coating of aqueous solutions of coordination compounds has been successfully implemented for the preparation of V_2O_5, Y_2O_3 and YVO_4 as well as luminescent Eu-doped YVO_4 films. The morphology of the films is highly influenced by the addition of (hydroxypropyl)methyl cellulose to the precursor solutions (c_{HPMC} = 4 g L^{-1}). In most cases, the polymer allows the formation of more uniform films, and the number of voids is clearly decreased. As expected, the spin-coating rate is confirmed as being a crucial parameter influencing the morphology and homogeneity of the films prepared by this method. It seems from this work that the addition of HPMC and a spin-coating rate of 3000 rpm is the best combination for obtaining continuous and dense inorganic films. Interestingly, it was evidenced by XRD analysis of the precursor films that, in some cases, there is a significant modification of crystal structures of the complexes in the films compared with the bulk structures. This is more than likely due to the high number of water molecules present in the complexes, which are intimately involved as a strong driving force for the crystallization process. The spin-coating procedure followed by the drying step probably has a significant impact on the number as well as on the spatial organization of these water molecules. Finally, it has been shown that this spin-coating preparation method induces a preferential orientation of crystallites within the films of V_2O_5 and YVO_4 with or without HPMC.

This work emphasizes, on the one hand, the poorly explored potential of edta complexes as molecular precursors for the preparation of films of pure and Eu-doped yttrium vanadate with luminescent properties and, on the other hand, the positive role played by the cellulosic derivative HPMC as additive inside a hybrid precursor for the same objective. It provides a detailed analysis of the potential of this quite simple chemical method, in aqueous medium and at comparatively moderate temperatures, for the synthesis of such materials, which are most often obtained under more severe or sophisticated conditions.

Experimental Section

Materials and Solvents: All products were analytical reagent grade and were used without further purification. Ammonium metavanadate, NH_4VO_3, ethanol and hydrogen peroxide (35 wt.-%) were supplied by Acros Organics. Yttrium nitrate hexahydrate, $Y(NO_3)_3 \cdot 6H_2O$, was purchased from Aldrich. Europium oxide, Eu_2O_3, was supplied by Alfa Aesar. Aqueous ammonia (28 wt.-%) and sulfuric acid (95%) were obtained from VWR. Ethylenediaminetetraacetic acid, H_4edta, and (hydroxypropyl)methyl cellulose, HPMC, were purchased from Fluka. The average number of methyl and hydroxypropyl groups can vary from one HPMC to another, and this polymer is characterized by a degree of substitution (DS), which characterizes the average number of hydroxy groups substituted per methyl or hydroxypropyl group. In addition, the molar substitution (MS) gives the average number of hydroxypropyl moieties per anhydroglucose unit. The cellulose derivative used in this work is characterized by a viscosity of a 2% aqueous solution, ca. 4000 mPa s, at 20 °C (DS = 19–24%, MS = 7–12%). Ultrapure water was purified by using an Elgastat Maxima system. The substrates for films were quartz Suprasil from Hellma. Syringe filters (polyethersulfone, porosity 0.45 μm, Pall Corporation) were used to filter the precursor solutions before coating.

Methods: UV/O_3 treatment using a Jelight's UVO-Cleaner 42 (λ = 254 nm) was applied to the quartz plates before coating. Spin coating of the precursor solutions was performed with a conventional spin coater (Spincoater Model P6700 Series). X-ray diffraction data were collected at room temperature with a Siemens D5000 diffractometer by using the Cu-K_α line (λ = 0.15418 nm). Scanning electron microscopy (SEM) was performed with a Gemini Digital Scanning Microscope 982 with an accelerating voltage of 1 kV. Raman spectra were recorded by using a confocal Renishaw Raman microscope at a wavelength of 780 nm. Photoluminescence analyses were collected with a Fluorolog-3 spectrometer from Jobin–Yvon-Spex (λ = 270 nm, integration time 1 s, increment 1 nm, slits 1 nm).

Preparation of the Coordination Compounds: The films were prepared by using a molecular precursor approach based on edta complexes, namely $(NH_4)[Y^{III}(edta)]\cdot 6H_2O$, $(NH_4)[Eu^{III}(edta)]\cdot 7.5H_2O$ and $(NH_4)_3[V^{V}(O)_2(edta)]\cdot 0.5H_2O$. The yttrium and europium complexes were synthesized from nitrates and oxides in basic medium. The vanadium precursor was obtained from NH_4VO_3 and H_4edta in basic medium. The synthetic pathways of these complexes are described in a previous paper.[16]

Preparation of the Films

Preparation of the Quartz Substrates: Before deposition, the quartz plates were cut into square pieces (1 cm × 1 cm) with a diamond cutter. The substrates were then sonicated in ethanol for 15 min and subsequently cleaned overnight in a piranha mixture [H_2SO_4/H_2O_2 (1:2, v/v)]. The plates were then thoroughly washed with ultrapure water (18.2 MΩ) and flushed with gaseous N_2. Finally, UV/O_3 treatment was applied for 15 min to obtain a static contact angle close to zero. The as-treated substrates were immediately used for film deposition.

Preparation of a Precursor Solution for Coating: The synthesized coordination compounds were dissolved in distilled water (10 mL) in appropriate proportions with final metal concentrations of 0.25 mol L^{-1}. For a series of samples, HPMC (0.04 g) was also added to the resulting clear solution.

Film Coating: The films were cast by placing several droplets of the 0.45 μm filtered precursor solution onto a treated quartz substrate resulting in a liquid film that completely covered the support (Figure 12). The quartz plate was then spun at 1000, 2000 or 3000 rpm for 60 s by using a conventional spin coater. The samples were dried at 110 °C for 15 min to form the precursor film. This precursor film was then calcined for 2 h at 600 °C for V_2O_5 and at 800 °C for

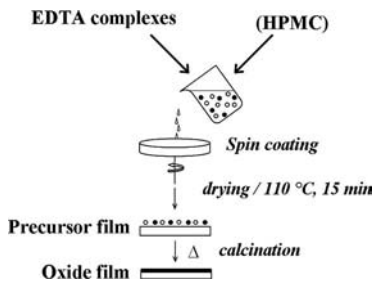

Figure 12. Preparation of the precursor and oxide films with or without HPMC.

Y_2O_3. For the YVO_4 films, a temperature of 600 °C was used when HPMC was added, and a temperature of 800 °C was used for YVO_4 samples prepared without HPMC.

Supporting Information (see footnote on the first page of this article): Additional Raman spectra, SEM images and XRD patterns of samples prepared under various conditions, together with the photoluminescence emission spectra and photo camera pictures of YVO_4:Eu films prepared with or without HPMC.

Acknowledgments

The authors thank the Belgian National Fund for Scientific Research (FNRS) for financial support. This work was also supported by a fellowship allotted to N. D. by the Fonds pour la Recherche dans l'Industrie et l'Agriculture (F.R.I.A.), Belgium and was performed within the framework of the Interuniversity Attraction Poles Program of the Belgian State, Belgian Science Policy (Project INANOMAT, P6/17). The authors are also grateful to Professor E. Gaigneaux for fruitful discussions.

[1] a) R. J. Gaboriaud, F. Pailloux, P. Guerin, F. Paumier, *Thin Solid Films* **2001**, *400*, 106–110; b) X. J. Wang, L. D. Zhang, J. P. Zhang, G. He, M. Liu, L. Q. Zhu, *Mater. Lett.* **2008**, *62*, 4235–4237.

[2] R. P. Rao, *Solid State Commun.* **1996**, *99*, 439–443.

[3] a) A. Kumar, P. Singh, N. Kulkarni, D. Kaur, *Thin Solid Films* **2008**, *516*, 912–918; b) H. Watanabe, K. Itoh, O. Matsumoto, *Thin Solid Films* **2001**, *386*, 281–285; c) Q. Su, W. Lan, Y. Y. Wang, X. Q. Liu, *Appl. Surf. Sci.* **2009**, *255*, 4177–4179.

[4] A. K. Levine, F. C. Palilla, *Appl. Phys. Lett.* **1964**, *5*, 118–120.

[5] a) G. R. Bai, H. Zhang, C. M. Foster, *Thin Solid Films* **1998**, *325*, 115–122; b) M. B. Korzenski, P. Lecoeur, B. Mercey, B. Raveau, *Chem. Mater.* **2001**, *13*, 1545–1551; c) W. Y. Kang, J. S. Park, D. K. Kim, K. S. Suh, *Bull. Korean Chem. Soc.* **2001**, *22*, 921–924; d) S. Yi, J. S. Bae, B. C. Choi, K. S. Shim, H. K. Yang, B. K. Moon, J. H. Jeong, J. H. Kim, *Opt. Mater.* **2006**, *28*, 703–708; e) F. Wang, S. N. Zhu, K. W. Cheah, *J. Appl. Phys.* **2006**, *99*, 096103-1–096103-3; f) K. S. Shim, H. K. Yang, B. K. Moon, J. H. Jeong, S. S. Yi, K. H. Kim, *Appl. Phys. A: Mater. Sci. Proc.* **2007**, *88*, 623–626; g) D. R. Milev, P. A. Atanasov, A. O. Dikovska, I. G. Dimitrov, K. P. Petrov, G. V. Avdeev, *Appl. Surf. Sci.* **2007**, *253*, 8250–8253; h) H. K. Yang, J. W. Chung, B. K. Moon, B. C. Choi, J. H. Jung, S. S. Yi, J. H. Kim, K. H. Kim, *Surf. Rev. Lett.* **2007**, *14*, 873–878; i) H. K. Yang, K. S. Shim, B. K. Moon, B. C. Choi, J. H. Jeong, S. S. Yi, J. H. Kim, *Thin Solid Films* **2008**, *516*, 5577–5581; j) H. X. Li, X. Wu, R. G. Song, *Mater. Charact.* **2008**, *59*, 1066–1069; k) H. K. Yang, J. W. Chung, B. K. Moon, B. C. Choi, J. H. Jeong, S. S. Yi, J. H. Kim, *Appl. Phys. A: Mater. Sci. Proc.* **2008**, *92*, 337–340; l) C. Cali, F. Cornacchia, A. Di Lieto, F. Marchetti, M. Tonelli, *Opt. Mater.* **2009**, *31*, 1331–1333; m) K. H. Jang, W. K. Sung, E. S. Kim, L. Shi, J. H. Jeong, H. J. Seo, *J. Lumin.* **2009**, *129*, 1853–1856.

[6] a) M. Yu, J. Lin, Y. H. Zhou, M. L. Pang, X. M. Han, S. B. Wang, *Thin Solid Films* **2003**, *444*, 245–253; b) M. Yu, J. Lin, Z. Wang, J. Fu, S. Wang, H. J. Zhang, Y. C. Han, *Chem. Mater.* **2002**, *14*, 2224–2231; c) S. Hirano, T. Yogo, K. Kikuta, W. Sakamoto, H. Koganei, *J. Am. Ceram. Soc.* **1996**, *79*, 3041–3044.

[7] a) J. Lin, M. Yu, C. Lin, X. Liu, *J. Phys. Chem. C* **2007**, *111*, 5835–5845; b) M. Yu, J. Lin, S. B. Wang, *Appl. Phys. A: Mater. Sci. Proc.* **2005**, *80*, 353–360.

[8] E. Bauer, A. H. Mueller, I. Usov, N. Suvorova, M. T. Janicke, G. L. N. Waterhouse, M. R. Waterland, Q. X. Jia, A. K. Burrell, T. M. McCleskey, *Adv. Mater.* **2008**, *20*, 4704–4707.

[9] H. Y. Xu, H. Wang, T. N. Jin, H. Yan, *Nanotechnology* **2005**, *16*, 65–69.

[10] W. Wang, Z. Cheng, P. Yang, Z. Hou, C. Li, G. Li, Y. Dai, J. Lin, *Adv. Funct. Mater.* **2011**, *21*, 456–463.

[11] R. M. Vanhardeveld, P. L. J. Gunter, L. J. Vanijzendoorn, W. Wieldraaijer, E. W. Kuipers, J. W. Niemantsverdriet, *Appl. Surf. Sci.* **1995**, *84*, 339–346.

[12] a) G. C. da Costa, A. Z. Simões, G. Gasparotto, M. A. Zaghette, B. Stojanovic, M. Cilense, J. A. Varela, *Mater. Res.* **2003**, *6*, 347–351; b) M. I. B. Bernardi, L. E. Soledade, I. A. Santos, E. R. Leite, E. Longo, J. A. Varela, *Thin Solid Films* **2002**, *405*, 228–233; c) L. J. Q. Maia, A. Ibanez, L. Ortega, V. R. Mastelaro, A. C. Hernandes, *J. Nanopart. Res.* **2008**, *10*, 1251–1262; d) J. M. Wang, Z. Lu, K. F. Chen, X. Q. Huang, N. Ai, J. Y. Hu, Y. H. Zhang, W. H. Su, *J. Power Sources* **2007**, *164*, 17–23; e) I. T. Weber, M. Garel, V. Bouquet, A. Rousseau, M. Guilloux-Viry, E. Longo, A. Perrin, *Thin Solid Films* **2005**, *493*, 139–145.

[13] a) Y. Y. Lua, X. P. Cao, B. R. Rohrs, D. S. Aldrich, *Langmuir* **2007**, *23*, 4286–4292; b) M. E. Pedley, P. B. Davies, *Vib. Spectrosc.* **2009**, *49*, 229–236; c) M. A. Repka, K. Gutta, S. Prodduturi, M. Munjal, S. P. Stodghill, *Eur. J. Pharm. Biopharm.* **2005**, *59*, 189–196; d) P. Sakellariou, R. C. Rowe, *Int. J. Pharm.* **1995**, *125*, 289–296.

[14] a) M. Devillers, O. Dupuis, A. Janosi, J. P. Soumillion, *Appl. Surf. Sci.* **1994**, *81*, 83–93; b) Y.-G. Choi, G. Sakai, K. Shimanoe, N. Miura, N. Yamazoe, *Chem. Sensors* **2001**, *17*, 288–290; c) W. Y. Chung, G. Sakai, K. Shimanoe, N. Miura, D. D. Lee, N. Yamazoe, *Sens. Actuators B* **2000**, *65*, 312–315; d) W. Y. Chung, *J. Mater. Sci. Mater. Electron.* **2001**, *12*, 591–596; e) Y. J. Kim, L. F. Francis, *J. Mater. Sci.* **1998**, *33*, 4423–4433.

[15] a) K. Traina, M. C. Steil, J. P. Pirard, C. Henrist, A. Rulmont, R. Cloots, B. Vertruyen, *J. Eur. Ceram. Soc.* **2007**, *27*, 3469–3474; b) H. Limage, K. Traina, C. Vanoerbeek, P. H. Duvigneaud, J. B. Soupart, R. Cloots, B. Vertruyen, *Proceedings of the 10th ECerS Conference, Berlin* (Eds.: J. G. Heinrich, C. Aneziris), Göller Verlag, Baden-Baden, **2007**, pp. 761–764.

[16] N. Deligne, V. Gonze, D. Bayot, M. Devillers, *Eur. J. Inorg. Chem.* **2008**, 896–902.

[17] a) B. S. Parajon-Costa, O. E. Piro, R. Pis-Diez, E. E. Castellano, A. C. Gonzalez-Baro, *Polyhedron* **2006**, *25*, 2920–2928; b) O. E. Piro, E. J. Baran, *J. Chem. Crystallogr.* **1997**, *27*, 475–479; c) J. C. Panitz, A. Wokaun, *J. Phys. Chem.* **1996**, *100*, 18357–18362.

[18] A. Klisinska, A. S. Mamede, E. M. Gaigneaux, *Catal. Today* **2007**, *128*, 145–152.

Received: March 29, 2011
Published Online: July 13, 2011

